
GNNInterpreter: A Probabilistic Generative Model-Level Explanation for Graph Neural Networks

Xiaoqi Wang

The Ohio State University
wang.5502@osu.edu

Han-Wei Shen

The Ohio State University
shen.94@osu.edu

Abstract

Recently, Graph Neural Networks (GNNs) have significantly advanced the performance of machine learning tasks on graphs. However, this technological breakthrough makes people wonder: how does a GNN make such decisions, and can we trust its prediction with high confidence? When it comes to some critical fields such as biomedicine, where making wrong decisions can have severe consequences, interpreting the inner working mechanisms of GNNs before applying them is crucial. In this paper, we propose a novel model-agnostic model-level explanation method for different GNNs that follow the message passing scheme, GNNInterpreter, to explain the high-level decision-making process of the GNN model. More specifically, with continuous relaxation of graphs and the reparameterization trick, GNNInterpreter learns a probabilistic generative graph distribution which produces the most representative graph for the target prediction in the eye of the GNN model. Compared with the only existing work, GNNInterpreter is more computationally efficient and more flexible in generating explanation graphs with different types of node features and edge features, without introducing another blackbox to explain the GNN and without requiring domain-specific knowledge. Additionally, the experimental studies conducted on four different datasets demonstrate that the explanation graph generated by GNNInterpreter can match the desired graph pattern when the model is ideal and reveal potential model pitfalls if there exist any.

1 Introduction

Graphs are widely used to model data in many applications such as chemistry, social science, transportation, etc. Since a graph is a unique non-Euclidean data structure, modeling graph data remained a challenging task until Graph Neural Networks (GNNs) emerged [1, 2, 3, 4]. As a powerful tool for representation learning on graph data, GNN achieved state-of-the-art performance on various different machine learning tasks on graphs. As the popularity of GNNs rapidly increases, people begin to wonder why one should trust this model and how the model makes decisions. However, the complexity of GNNs prevents humans from interpreting the underlying mechanism in the model. The lack of self-explainability becomes a serious obstacle for applying GNNs to real-world problems, especially those when making wrong decisions may incur an unaffordable cost.

Explaining deep learning models on text or image data[5, 6, 7, 8, 9] has been well-studied. However, the explainability of deep learning models on graphs is still less explored. Compared with explaining deep learning models on text or image data, explaining deep graph models is a more challenging

task for several reasons [10]: (i) since a graph is not a grid-structured data like the image or text, the locality information of nodes is absent and each node has a varying number of neighbors[11], (ii) the adjacency matrix representing the topological information has only discrete values, which cannot be directly optimized via gradient-based methods[12], and (iii) graph data structure is heterogeneous in nature with different types of node features and edge features, which makes developing a one-size-fits-all explanation method for GNNs to be even more challenging.

In recent years, explaining GNNs has aroused great interest and thus many research works have been conducted. The existing works can be classified into two categories: instance-level explanations [13, 14, 15] and model-level explanations [16]. Specifically, instance-level explanation methods attempt to interpret the model prediction for a given graph instance, whereas model-level explanation methods aim at understanding the general behavior of the model not specific to any particular graph instance. However, if the ultimate goal is to examine the model reliability, instance-level methods are very time-consuming because one will need to examine many instances one by one to draw a rigorous conclusion about the model reliability. Conversely, the model-level explanation method can directly explain the underlying mechanism inside the blackbox (GNN) for a target prediction, which is much less time-consuming and more informative about the general decision-making process of the model.

In this paper, we propose a novel model-level explanation method, GNNInterpreter, which generates explanations about the high-level decision-making process of GNNs. Specifically, we learn a generative probabilistic graph distribution via continuous relaxation of graphs and reparameterization trick such that the graphs sampled from the generative distribution represent the most discriminative features the GNN tries to detect when making a certain prediction. Thus, by analyzing the characteristics of the explanation graphs, the true belief inside the GNN model regarding the target prediction can be revealed. In addition, GNNInterpreter is a general approach to generating explanation graphs with different types of node features and edge features for explaining different GNNs which follows the message passing scheme. We quantitatively and qualitatively evaluated the efficiency and effectiveness of GNNInterpreter on four different datasets including synthetic datasets and public real-world dataset. The experimental results show that GNNInterpreter can precisely find the ideal topological structure for the target prediction if the explained model is ideal, and manifest the potential pitfalls in the model decision-making process if there exists any.

To the best of our knowledge, there is only one existing work about the model-level explanation for GNNs, called XGNN[16]. The quantitative and qualitative evaluation result shows that the explanation graphs generated by GNNInterpreter is more representative regarding the target class than the graphs generated by XGNN. Additionally, GNNInterpreter has the following advantages compared with XGNN:

- GNNInterpreter is a numerical optimization approach without introducing another blackbox to explain GNNs, unlike XGNN which trains a deep learning model to explain GNNs.
- GNNInterpreter is a more general approach that can generate explanation graphs with different types of node features and edge features, whereas XGNN cannot generate graphs with continuous node features or any type of edge features.
- GNNInterpreter is more flexible to explain different GNN models without the need of having domain-specific knowledge for the specific task, whereas XGNN requires domain-specific knowledge to manually design the reward function for the reinforcement learning agent.
- GNNInterpreter is more computationally efficient because GNNInterpreter only takes less than a minute to explain one class in a GNN model, which is about 10 times faster than training a deep reinforcement learning agent as in XGNN.

2 Related Work

Graph Neural Network. Unlike images and texts, modeling graph data is a very challenging task due to the unique characteristic of graphs. Many interesting researches have been conducted to extend the previously existing deep learning algorithms to graph data, which gives rise to the emergence of GNNs. GNNs have achieved remarkable success in different machine learning tasks including graph classification[17], node classification[18], and link prediction[19]. There exists a variety of GNN models [20, 21, 22, 23, 24] but they often share a common idea of message passing as

described in section 3 but with different time complexity[25]. More importantly, GNNInterpreter is model-agnostic in a way that it can interpret different GNNs following the message passing scheme.

Instance-Level Explanation of GNN. Encouraged by the success of explaining deep neural networks on image or text data, the first instance-level explanation method of GNNs[26] emerged in 2019. Since then, a multitude of instance-level explanation methods of GNNs has been proposed in the past few years. According to a recent survey[10], these instance-level explanation methods can be classified into four categories: gradient-based methods[26, 27], perturbation-based methods[14, 13, 28], decomposition methods[26, 27, 29], and surrogate methods[15, 30, 31]. These four categories all attempt to explain how a GNN model makes such a prediction for a specific input instance. However, if the ultimate goal is to validate whether this model is trustworthy, it is very time-consuming to manually check the instance-level explanation for many graph instances one by one before we can make any rigorous conclusion about the model reliability.

Model-Level Explanation Method of GNN. Unlike instance-level explanation methods, model-level explanation methods aim to explain the general behavior of a model without respect to any specific input. To the best of our knowledge, XGNN[16] is the only existing work focusing on the model-level explanation of GNN. Similar to the most of model-level explanation methods for other deep learning model [5, 32], XGNN and GNNInterpreter have a common goal which is generating an explanation graph to maximize the likelihood of the target prediction being made by the GNN model. However, XGNN adopts a completely different approach. To be more concrete, given a target class c , XGNN trains a deep graph generator f_c in a reinforcement learning setting. During the training, f_c will propose adding one edge to the current input graph for each step. After training, the graph generator f_c can predict the explanation graph which maximizes the score of class c , given a pre-specified number of steps. Besides, it incorporates hand-crafted graph rules into the reward function such that f_c can consider these rules while providing explanations. However, specifying these graph rules requires domain-specific knowledge about the tasks. XGNN also has a limitation that it can only generate explanation graphs with a single categorical node feature or no node feature. In other words, it cannot generate explanation graphs with any types of edge features or continuous node features. Unlike XGNN, GNNInterpreter is more general to generate explanation graphs with different types of node features and edge features, without requiring domain-specific knowledge. Additionally, GNNInterpreter is more computationally efficient in providing explanations per class, without introducing another blackbox to explain GNNs.

3 Background

Notations. A graph is represented as $G = (\mathbf{V}, \mathbf{E})$, where \mathbf{V} and \mathbf{E} are the sets of nodes and edges. Besides, the number of edges and nodes are denoted as M and N respectively. The topological information of a graph is described by an adjacency matrix $\mathbf{A} \in \{0, 1\}^{N \times N}$ where $a_{ij} = 1$ if there exists an edge between node i and node j , and $a_{ij} = 0$ otherwise. In addition, the node feature matrix $\mathbf{X} \in \mathbb{R}^{N \times k_V}$ and edge feature matrix $\mathbf{Z} \in \mathbb{R}^{M \times k_E}$ represent the features for N nodes and M edges.

Graph Neural Networks. In general, the high-level idea of GNN is message passing. For each layer, it aggregates information from neighboring nodes to learn the representation of each node. For hidden layer i , the message passing operation can be written as

$$\begin{cases} \mathbf{H}^0 &= \mathbf{X}, \\ \mathbf{H}^i &= f(\mathbf{H}^{i-1}, \mathbf{A}, \mathbf{Z}), \end{cases} \quad (1)$$

where $\mathbf{H}^i \in \mathbb{R}^{N \times F^i}$ is the hidden node representation output from i^{th} layer and F^i is the output feature dimension. The propagation rule f can be decomposed into three components: computing the messages according to the node embedding at the previous layer \mathbf{H}^{i-1} , aggregating the messages from neighboring nodes, and updating the hidden representation \mathbf{H}^i for each node based upon the aggregated message. It is worth mentioning that GNNInterpreter can explain different GNNs that follow this message passing scheme.

4 GNNInterpreter

In this paper, we propose a model-level explanation method, GNNInterpreter, which is capable of disclosing the high-level decision-making process of the model for the purpose of examining

model reliability. GNNInterpreter is a numerical optimization approach that is model-agnostic for explaining different GNNs following the message passing scheme, and can generate explanation graphs with different types of edge features and node features without the need of domain-specific knowledge for specific tasks. Specifically, via the technique of continuous relaxation of graphs and reparametrization trick, GNNInterpreter learns a probabilistic generative graph distribution which captures the discriminative features the GNN tries to detect when making a certain prediction.

4.1 Learning Objective

To reveal the high-level decision-making process of the model, one effective approach is to construct an explanation graph that can trigger a specific response from the model as much as possible. Similar to the most of model-level explanation methods for other deep learning model [5, 32], the explanation for GNNs can be obtained by maximizing the likelihood of the explanation graph G being predicted as a target class by the GNN model. However, solely maximizing the likelihood without constraints may not necessarily result in meaningful explanations. This is because a local maxima in the objective landscape may lie outside of the training data distribution. The explanation yielded from this type of maxima are mathematically legitimate but may provide no meaningful insights on how the model actually reasons over the true data distribution. Especially when there exists domain-specific knowledge that restricts the validity of the data, the explanations are expected to stay inside the hard boundary of the true data distribution. XGNN[16] addresses this problem by manually specifying a set of graph rules and evaluating the validity of explanation graphs according to the specified rules as a part of the reward function for the reinforcement learning agent. The essential goal is to confine the distribution of the explanation graphs to the domain-specific boundary. Nevertheless, manually specifying rules not only is tedious and time-consuming, but also requires domain expertise which is not always available. Moreover, in many cases, the rules over data distribution can not even be programmatically specified. Therefore, we propose to leverage the learned abstract knowledge by the GNN itself to prevent the explanation from deviating from the true data distribution. This can be achieved by maximizing the similarity between the explanation graph embedding and the average embedding of the target class. Thus, we mathematically formulate our learning objective as follows,

$$\max_G L(G) = \max_{\mathbf{A}, \mathbf{Z}, \mathbf{X}} L(\mathbf{A}, \mathbf{Z}, \mathbf{X}) = \max_{\mathbf{A}, \mathbf{Z}, \mathbf{X}} \phi_c(\mathbf{A}, \mathbf{Z}, \mathbf{X}) + \mu \text{sim}_{\cos}(\psi(\mathbf{A}, \mathbf{Z}, \mathbf{X}), \bar{\psi}_c) \quad (2)$$

where L is the objective function; ϕ_c is the scoring function before softmax corresponding to the class of interest c , predicted by the explained GNN; ψ is the graph embedding function of the explained GNN; $\bar{\psi}_c$ is the average graph embedding for all graphs belonging to class c in the training set; sim_{\cos} denotes the cosine similarity; and μ is a hyper-parameter representing the weight factor.

Given the learning objective defined above, one possible approach to obtain the explanation graph is that we can adopt the gradient ascent to iteratively update the explanation graph G toward maximizing the learning objective. However, this approach cannot be directly applied here because the discrete adjacency matrix \mathbf{A} encoding the graph topology is non-differentiable, namely $\nabla_{\mathbf{A}} L(\mathbf{A}, \mathbf{Z}, \mathbf{X})$ does not exist. Therefore, in order to adopt the gradient ascent method, \mathbf{A} need to be relaxed to a continuous variable. In addition, if the training graphs of the GNN model have discrete edge features or discrete node features, then \mathbf{Z} and \mathbf{X} are also required to be relaxed to the continuous domain such that $\nabla_{\mathbf{Z}} L(\mathbf{A}, \mathbf{Z}, \mathbf{X})$ and $\nabla_{\mathbf{X}} L(\mathbf{A}, \mathbf{Z}, \mathbf{X})$ exist. Given that the continuous edge features and continuous node features do not require any special accommodation to adopt the gradient ascent, we will only discuss how to learn a continuously relaxed explanation graph with discrete edge features and discrete node features in the following sections.

4.2 Learning Generative Graph Distribution

To learn a probabilistic generative graph distribution such that the graph drawn from this distribution can maximize the learning objective, two assumptions have been made about the explanation graph. The first assumption is that the graph is a Gilbert random graph [33] in which every possible edge occurs independently with probability $0 < p < 1$. The second assumption is that the features for each node and edge are independently distributed. Given these two assumptions, the probability distribution of the graph G , a random graph variable, can be factorized as

$$P(G) = \prod_{i \in \mathbf{V}} P(x_i) \cdot \prod_{(i,j) \in \mathbf{E}} P(z_{ij}) P(a_{ij}) \quad (3)$$

where $a_{ij} = 1$ when there exists an edge between node i and j and $a_{ij} = 0$ otherwise, z_{ij} denotes the edge feature between node i and j , and x_i represents the node feature of node i .

Intuitively, a_{ij} can be modeled as a Bernoulli distribution in which the probability of success θ_{ij} represents the probability of an edge existing between node i and j in G . For the discrete edge feature z_{ij} and the discrete node feature x_i , we can assume that z_{ij} and x_i follow a Categorical distribution, a generalized Bernoulli distribution, with the parameter specifying the probability of each possible outcome for the categorical node feature and the categorical edge feature. In summary, the probability distribution of a_{ij} , x_i and z_{ij} can be written as

$$\begin{cases} a_{ij} \sim \text{Bernoulli}(\theta_{ij}), & \text{for } a_{ij} \in \mathbf{A} \text{ and } \theta_{ij} \in \Theta \\ z_{ij} \sim \text{Categorical}(\mathbf{q}_{ij}), & \text{for } z_{ij} \in \mathbf{Z} \text{ and } \mathbf{q}_{ij} \in \mathbf{Q} \\ x_i \sim \text{Categorical}(\mathbf{p}_i), & \text{for } x_i \in \mathbf{X} \text{ and } \mathbf{p}_i \in \mathbf{P} \end{cases} \quad (4)$$

where $\|\mathbf{q}_{ij}\|_1 = 1$ and $\|\mathbf{p}_i\|_1 = 1$. We define the number of edge categories $k_E = \dim(\mathbf{q}_{ij})$ and the number of node categories $k_V = \dim(\mathbf{p}_i)$. Thus, to learn the probabilistic distribution for explanation graphs, we can rewrite the learning objective as

$$\max_G L(G) = \max_{\Theta, \mathbf{Q}, \mathbf{P}} \mathbb{E}_{G \sim P(G)} [\phi_c(\mathbf{A}, \mathbf{Z}, \mathbf{X}) + \mu \text{sim}_{\cos}(\psi(\mathbf{A}, \mathbf{Z}, \mathbf{X}), \bar{\psi}_c)]. \quad (5)$$

4.3 Continuous Relaxation with Reparameterization Trick

To adopt gradient ascent over the learning objective function with respect to a graph with the discrete edge feature z_{ij} and the discrete node feature x_i , we relax a_{ij} , z_{ij} and x_i to continuous random variables \tilde{a}_{ij} , \tilde{z}_{ij} and \tilde{x}_i , respectively. Specifically, a_{ij} is relaxed to $\tilde{a}_{ij} \in [0, 1]$; z_{ij} is relaxed to $\tilde{z}_{ij} \in [0, 1]^{k_E}$, $\|\tilde{z}_{ij}\|_1 = 1$; and x_i is relaxed to $\tilde{x}_i \in [0, 1]^{k_V}$, $\|\tilde{x}_i\|_1 = 1$. Given that the Concrete distribution[34] is a family of continuous versions of Categorical random variables with closed form density, the distribution of continuously relaxed \tilde{a}_{ij} , \tilde{z}_{ij} and \tilde{x}_i can be written as

$$\begin{cases} \tilde{a}_{ij} \sim \text{BinaryConcrete}(\omega_{ij}, \tau_a), & \text{for } \tilde{a}_{ij} \in \tilde{\mathbf{A}} \text{ and } \omega_{ij} \in \Omega \\ \tilde{z}_{ij} \sim \text{Concrete}(\eta_{ij}, \tau_z), & \text{for } \tilde{z}_{ij} \in \tilde{\mathbf{Z}} \text{ and } \eta_{ij} \in \mathbf{H} \\ \tilde{x}_i \sim \text{Concrete}(\xi_i, \tau_x), & \text{for } \tilde{x}_i \in \tilde{\mathbf{X}} \text{ and } \xi_i \in \Xi \end{cases} \quad (6)$$

where $\tau \in (0, \infty)$ is the hyper-parameter representing the temperature, $\omega_{ij} = \log(\theta_{ij}/(1 - \theta_{ij}))$, $\eta_{ij} = \log \mathbf{q}_{ij}$, and $\xi_i = \log \mathbf{p}_i$. As the temperature approaches zero, the Concrete distribution is mathematically equivalent to the Categorical distribution.

However, in order to learn the generative explanation graph distribution, the sampling function for sampling \tilde{a}_{ij} , \tilde{z}_{ij} and \tilde{x}_i from the Concrete distribution is required to be differentiable. Thus, the reparameterization trick is adopted to approximate the sampling procedure of \tilde{a}_{ij} , \tilde{z}_{ij} and \tilde{x}_i by a differentiable function. Given an independent random variable $\epsilon \sim \text{Uniform}(0,1)$, the sampling function with the reparameterization trick is as follows,

$$\begin{cases} \tilde{a}_{ij} = \text{sigmoid}((\omega_{ij} + \log \epsilon - \log(1 - \epsilon)) / \tau_a) \\ \tilde{z}_{ij} = \text{softmax}((\eta_{ij} - \log(-\log \epsilon)) / \tau_z) \\ \tilde{x}_i = \text{softmax}((\xi_i - \log(-\log \epsilon)) / \tau_x) \end{cases} \quad (7)$$

Given this reparameterization trick, we can draw a sample \tilde{a}_{ij} as an approximation of a_{ij} , where the probability of \tilde{a}_{ij} to be close to 1 is the same as the probability of a_{ij} to equal 1 and vice versa. Specifically, $P(\tilde{a}_{ij} \rightarrow 1) = 1 - P(\tilde{a}_{ij} \rightarrow 0) = P(a_{ij} = 1) = \theta_{ij} = \text{sigmoid}(\omega_{ij})$. Similarly, \tilde{z}_{ij} and \tilde{x}_i drawn from the Concrete distribution as in Equation 7 is an approximation of z_{ij} and x_i . Therefore, the learning objective with continuous relaxation and reparameterization trick can be approximated by the Monte Carlo method with K samples,

$$\max_{\Theta, \mathbf{Q}, \mathbf{P}} \mathbb{E}_{G \sim P(G)} [L(\mathbf{A}, \mathbf{Z}, \mathbf{X})] \approx \max_{\Omega, \mathbf{H}, \Xi} \mathbb{E}_{\epsilon \sim U(0,1)} [L(\tilde{\mathbf{A}}, \tilde{\mathbf{Z}}, \tilde{\mathbf{X}})] \approx \max_{\Omega, \mathbf{H}, \Xi} \frac{1}{K} \sum_{k=1}^K L(\tilde{\mathbf{A}}, \tilde{\mathbf{Z}}, \tilde{\mathbf{X}}). \quad (8)$$

Algorithm 1: Generate Explanation Graphs Using GNNInterpreter

```
1 Calculate the average graph embedding  $\bar{\psi}_c$  from the training data of GNN model.
2 Initialize latent parameters  $\Omega$ ,  $\mathbf{H}$ , and  $\Xi$ .
3 while not converged do
4   for  $k \leftarrow 1 \dots K$  do
5     Using the reparameterization trick, sample  $\tilde{\mathbf{A}}, \tilde{\mathbf{E}}, \tilde{\mathbf{X}}$  with Equation 7.
6     Obtain the class score  $s_c^{(k)} \leftarrow \phi_c(\tilde{\mathbf{A}}, \tilde{\mathbf{E}}, \tilde{\mathbf{X}})$ .
7     Obtain the graph embedding  $\mathbf{h}_c^{(k)} \leftarrow \psi_c(\tilde{\mathbf{A}}, \tilde{\mathbf{E}}, \tilde{\mathbf{X}})$ .
8   end
9   Calculate  $L \leftarrow \frac{1}{K} \sum_{k=1}^K [s_c^{(k)} + \mu \text{sim}_{\cos}(\mathbf{h}_c^{(k)}, \bar{\psi}_c)]$  with the regularization terms.
10  Calculate  $\nabla_{\Omega} L$ ,  $\nabla_{\mathbf{H}} L$ , and  $\nabla_{\Xi} L$ , then update  $\Omega$ ,  $\mathbf{H}$ , and  $\Xi$  using gradient ascent.
11 end
12 return  $G = (\mathbf{A}, \mathbf{E}, \mathbf{X})$ , where  $\mathbf{A}, \mathbf{E}, \mathbf{X}$  are sampled with Equation 4.
```

4.4 The Generalizability of GNNInterpreter

GNNInterpreter can generate explanation graphs with different types of node features and edge features if needed. If the node feature or edge feature is continuous, $\nabla_{\mathbf{X}} L(\mathbf{A}, \mathbf{Z}, \mathbf{X})$ and $\nabla_{\mathbf{Z}} L(\mathbf{A}, \mathbf{Z}, \mathbf{X})$ naturally exist, then we only need to relax the adjacency matrix \mathbf{A} to a continuous random variable following the Binary Concrete distribution. Additionally, unlike XGNN which can only learn graphs with a single categorical node feature, the number of edge features and node features are not limited in GNNInterpreter.

GNNInterpreter can explain different GNNs following the message passing scheme. In the original message passing scheme, messages are aggregated from their neighbors to update the node embedding at the current layer. To adapt the message passing scheme for GNNInterpreter, messages are passed from all the other nodes but each message is weighted by $\theta_{ij} = \text{sigmoid}(\omega_{ij})$. Therefore, if θ_{ij} approaches to 1, meaning that node i and node j are highly likely to be the neighbor, the message passed between them will be the same as in the original message passing scheme. With this small modification of message passing, GNNInterpreter can be easily applied to different GNNs following the message passing scheme. In order to facilitate optimization and ensure that the explanation graphs are constrained to desired properties, we apply multiple regularization terms to the latent parameters, whose detailed formulations are presented in Appendix. Also, the training procedure of GNNInterpreter is shown in algorithm 1.

5 Experimental Study

In order to comprehensively assess the effectiveness of GNNInterpreter, we carefully design the experimental study conducted on 4 different datasets so that it not only demonstrates our flexibility of generating explanation graphs with various types of features but also manifests our capability of explaining different GNNs. More specifically, we train a GNN classifier for each dataset and adopt GNNInterpreter to explain the GNN models. In addition, we quantitatively and qualitatively evaluate the efficacy of GNNInterpreter compared to XGNN[16]. Note that the experimental settings, the generation process of synthetic dataset, and engineering details of GNNs are illustrated in Appendix.

Table 1: The statistics of datasets and some technical details about their corresponding GNN models.

Dataset	# of Classes	Node Features	Edge Features	Average # of Edges	Average # of Nodes	GNN Type	GNN Test Accuracy
MUTAG[35]	2	✓		19.79	17.93	GCN[20]	0.9468
Cyclicity	3		✓	52.76	52.51	NNConv[21]	0.9921
Motif	5	✓		77.36	57.07	GCN[20]	0.9964
Shape	5			71.86	30.17	GCN[20]	0.9725

5.1 Datasets

Synthetic Dataset. We synthetically generate 3 datasets which are Cyclicity, Motif, and Shape (see Table 1). (1) In **Cyclicity**, the graphs have an categorical edge feature with 2 possible values: green or

red. There are 3 class labels in Cyclicity, which are Red-Cyclic graphs, Green-Cyclic graphs, and Acyclic graphs. Specifically, a graph will be labeled as a green/red cyclic graph only if it is cyclic and the edges forming that cycle are all green/red. If a graph is categorized as Acyclic, then it either does not contain a cycle at all or contains a cycle but with a mixture of green and red edges. (2) The graphs in **Motif** are labeled according to whether they contain a certain motif. There are 4 motifs (i.e., House, House-X, Complete-4, and Complete-5) will possibly appear in the graphs and each motif corresponds to one class label. There is another class that contains the graphs without any special motif. Besides, each node in the graphs has a categorical node feature with 5 possible values: red, orange, green, blue, and purple. (3) **Shape** contains 5 classes of graphs: Lollipop, Wheel, Grid, Star, and Others. In all the classes except the Others class, graphs are generated with the corresponding shape. For the Others class, graphs are randomly generated without any special topology.

Real-world Dataset. **MUTAG**[35] is a real-world dataset with 2 classes: Mutagen and Nonmutagen. Each graph is categorized according to its mutagenic effect on the Gram-negative bacterium *S. typhimurium*[36]. Given the fact that the molecules with more NO_2 are more likely to mutate, the graphs in the Mutagen class tend to have more NO_2 than those in the Nonmutagen class. Also, Mutagen class and Nonmutagen class share a common feature which is rings of carbon atoms.

5.2 Results

To investigate whether GNNInterpreter can truly explain the high-level decision-making process, we evaluate GNNInterpreter both quantitatively and qualitatively. Following XGNN[16], the class probability of the explanation graphs predicted by the GNN is adopted as the quantitative metric since GNNInterpreter and XGNN share a common objective of maximizing the target class score (Table 2). Also, to qualitatively evaluate GNNInterpreter, we present the explanation graphs per class for all datasets, which are all predicted as the target class with the class probability of 1 (Figure 8).

Table 2: The quantitative results for 4 datasets. As the quantitative metric, we compute the average class probability of 1000 explanation graphs and the standard deviation of them for every class in all 4 datasets. In addition, the average training time per class of training 100 different GNNInterpreter and XGNN models, is also included for efficiency evaluation.

Dataset [Method]	Predicted Class Probability by GNN				Training Time Per Class
MUTAG [XGNN]	Mutagen	Nonmutagen			128 s
	0.986 ± 0.057	0.991 ± 0.083			
MUTAG [Ours]	Mutagen	Nonmutagen			12 s
	1.000 ± 0.000	1.000 ± 0.000			
Cyclicity [Ours]	Red Cyclic	Green Cyclic	Acyclic		49 s
	1.000 ± 0.000	1.000 ± 0.000	1.000 ± 0.000		
Motif [Ours]	House	House-X	Complete-4	Complete-5	83 s
	0.918 ± 0.268	0.999 ± 0.032	1.000 ± 0.000	0.998 ± 0.045	
Shape [Ours]	Lollipop	Wheel	Grid	Star	24 s
	0.742 ± 0.360	0.989 ± 0.100	0.996 ± 0.032	1.000 ± 0.000	

Since XGNN is the only existing model-level explanation method for GNNs, we compare GNNInterpreter with XGNN quantitatively and qualitatively. However, given that XGNN cannot generate explanation graphs with edge features, XGNN is not applicable to the Cyclicity dataset. For Motif and Shape, we attempted to adopt XGNN to explain the corresponding GNNs, but the explanation results were not acceptable even after our extensive efforts of trial-and-error on XGNN. Therefore, for a fair comparison, we only present the evaluation results of XGNN on the GNN trained on MUTAG, with the same hyper-parameter settings for MUTAG as they discussed in their paper.

MUTAG. The quantitative evaluation in Table 2 shows that all explanation graphs generated by GNNInterpreter are classified correctly with 100% probability for both classes, which indicates the absolute belief of GNN in GNNInterpreter explanations. On the contrary, the GNN is more hesitant or diffident when classifying the XGNN explanation graphs for both classes. Speaking of time efficiency, for explaining the same GNN model trained on MUTAG, *training a GNNInterpreter model is about 10 times faster than training an XGNN model on average*. In Figure 8, the GNNInterpreter explanation for Mutagen class contains 5 repeated NO_2 whereas the GNNInterpreter explanation for Nonmutagen class does not contain O atom at all, which are perfectly aligned with our background knowledge about the MUTAG dataset mentioned in subsection 5.1. In contrast, the XGNN explanation for Mutagen class only contains a single NO_2 , which is a less accurate or ideal explanation than ours.

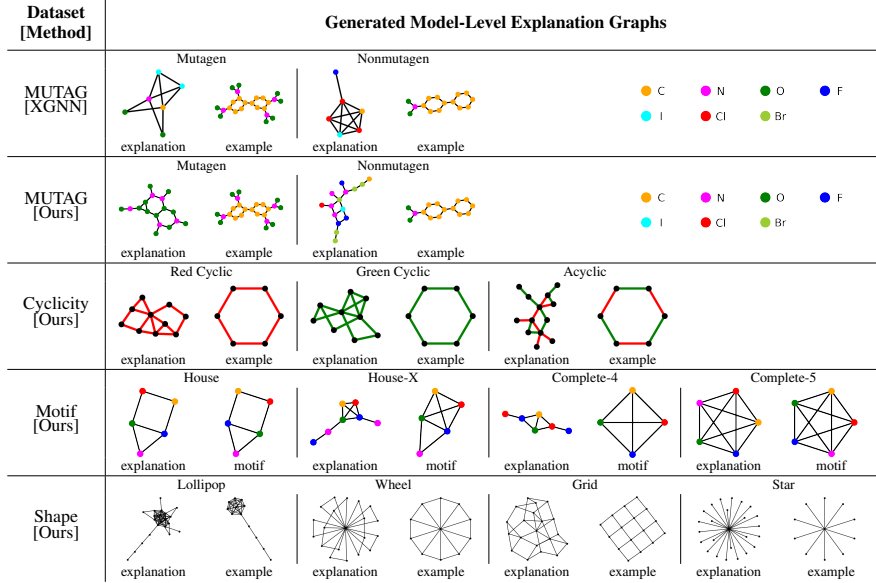


Figure 1: The qualitative results for 4 datasets. For each class in all datasets, the explanation graph with the class probability of 1 predicted by the GNNs is displayed on the left; as a reference, the example graph selected from the training data of the GNNs or the motif is displayed on the right. The different colors in the nodes and edges represent different values in the node feature and edge feature.

Cyclicity. In Table 2, the average class probability for all three classes is 1.00 with 0 standard deviation, which means that we can consistently generate the most representative explanation graphs in terms of the explained GNN for all three classes. Besides, in Figure 8, the explanation graphs for Red Cyclic and Green Cyclic only contain multiple red cycles and multiple green cycles, respectively; the explanation graph for Acyclic does not contain any cycle with homogeneous edge colors. These explanations are very accurate and reveal a pattern that the *more occurrences of the discriminative feature for the corresponding class (i.e., red cycle, green cycle, and cycle with heterogeneous edge color, respectively) substantially boost the confidence of the GNN during the decision-making process.*

Motif. In Table 2, the average class probability for all 4 classes are equal to or very close to 1 with zero or small standard deviation, which is much higher than 0.2 (the baseline probability of random guess for a classification task with 5 classes). Also, in Figure 8, the explanation graphs for House and Complete-5 class match the exact motif. Even though the explanation graphs for House-X and Complete-4 do not match the exact motif, it still obtains the class probabilities of 1. According to this, we speculate the true belief inside the GNN is that: in House-X graphs, orange node and red node should have 3 neighbors except purple node, green node and blue node should have 4 neighbors in different color; in Complete-4 graphs, every node should have 3 neighbors in different color. *We can see that the GNN with a high test accuracy of 0.9964 (Table 2) actually perceives the wrong motifs as the House-X and Complete-4, which can potentially result in misclassification for unseen graphs.*

Shape. The average class probability for Wheel, Grid, and Star are equal to or very close to 1, whereas the average class probability for Lollipop is 0.742. However, 0.742 is still a reasonably high probability than 0.2 (the baseline probability of random guess for 5 classes). Qualitatively speaking, the explanation graphs for all 4 classes presented in Figure 8 are almost consistent with the desired graph topology. Nonetheless, it also discloses some interesting findings regarding the high-level decision-making process of the GNN. For Wheel and Grid class, the explanation graphs are not very perfect but with the predicted class probability of 1. Accordingly, we infer the true belief inside the GNN is that: the discriminative features of Wheel graph and Grid graph are a single common vertex shared by multiple triangles and multiple polygons sharing some common edges, respectively. *These might become a potential model pitfall because, for example, the GNN will be easily tricked by a non-wheel graph in which there exists a common vertex shared by multiple triangles.*

Verification Study. Since the ground truth model-level explanation graphs are unknown, the correctness of our analysis regarding these potential GNN pitfalls cannot be directly justified. Therefore,

to verify the correctness, we conduct controlled experimental studies to test how the GNN behaves on some carefully chosen input graphs with specific misleading patterns. Specifically, by observing the commonality among our explanations for House-X and the ground truth motif, we speculate the true belief inside the explained GNN regarding the House-X class is that "orange node and red node should have 3 neighbors except purple node, green node and blue node should have 4 neighbors in different color". We found 9 plausible motifs (including the ground truth House-X) which satisfy this rule, as shown in Figure 2. Given a fixed set of 5000 base graphs, each of the 9 different motifs are attached to the same node of each base graphs respectively. As a result, we obtain 9 sets of graphs each of which contains 5000 graphs corresponding to one of the motifs. For each motif set, the classification results are presented in Table 10. We can see that *motif 1-8 successfully fool the explained GNN because a large portion of the non-House-X graphs are incorrectly classified as House-X*. This verification result strongly supports our qualitative analysis regarding the potential model pitfall for House-X class. The verification studies for more classes are presented in Appendix.

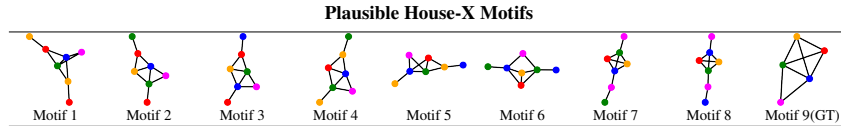


Figure 2: The ground truth class label for motif 1-8 and motif 9 is Others and House-X, respectively.

	Motif 1	Motif 2	Motif 3	Motif 4	Motif 5	Motif 6	Motif 7	Motif 8	Motif 9 (GT)
Others	1434	2251	1808	1970	2183	597	1682	1696	10
House	0	0	0	0	0	0	0	0	0
House-X	3566	2749	3192	3030	2817	4403	3318	3304	4990
Complete-4	0	0	0	0	0	0	0	0	0
Complete-5	0	0	0	0	0	0	0	0	0

Table 3: The classification results of plausible House-X motifs.

6 Conclusion

We propose a novel model-level explanation method for GNNs, GNNInterpreter. Via continuous relaxation of graphs and reparameterization trick, it learns a probabilistic generative graph distribution to depict the true belief inside the GNN model about the target class. The quantitative result shows that GNNInterpreter can consistently generate the most representative explanation graphs in the eye of GNN. By analyzing the explanation graphs qualitatively, we can precisely infer the high-level decision-making process of the GNN and even reveal some potential model pitfalls if there exist any. We outperform the only existing model-level explanation method for GNNs, XGNN, both quantitatively and qualitatively. Lastly, the outstanding generalizability of GNNInterpreter and superior time efficiency make GNNInterpreter more practical in real-world applications.

References

- [1] M. Defferrard, X. Bresson, and P. Vandergheynst, "Convolutional neural networks on graphs with fast localized spectral filtering," in *Advances in Neural Information Processing Systems*, 2016.
- [2] W. Hamilton, R. Ying, and J. Leskovec, "Inductive representation learning on large graphs," 06 2017.
- [3] S. Cao, W. Lu, and Q. Xu, "Deep neural networks for learning graph representations," ser. AAAI'16. AAAI Press, 2016, p. 1145–1152.
- [4] W. Yu, C. Zheng, W. Cheng, C. C. Aggarwal, D. Song, B. Zong, H. Chen, and W. Wang, "Learning deep network representations with adversarially regularized autoencoders," in *Proceedings of the 24th ACM SIGKDD International Conference on Knowledge Discovery & Data Mining*, ser. KDD '18. New York, NY, USA: Association for Computing Machinery, 2018, p. 2663–2671. [Online]. Available: <https://doi.org/10.1145/3219819.3220000>
- [5] K. Simonyan, A. Vedaldi, and A. Zisserman, "Deep inside convolutional networks: Visualising image classification models and saliency maps," *CoRR*, vol. abs/1312.6034, 2014.

- [6] R. R. Selvaraju, A. Das, R. Vedantam, M. Cogswell, D. Parikh, and D. Batra, “Grad-cam: Visual explanations from deep networks via gradient-based localization,” *International Journal of Computer Vision*, vol. 128, pp. 336–359, 2019.
- [7] J. Zhang, Z. L. Lin, J. Brandt, X. Shen, and S. Sclaroff, “Top-down neural attention by excitation backprop,” *International Journal of Computer Vision*, vol. 126, pp. 1084–1102, 2017.
- [8] A. Binder, G. Montavon, S. Lapuschkin, K.-R. Müller, and W. Samek, “Layer-wise relevance propagation for neural networks with local renormalization layers,” in *ICANN*, 2016.
- [9] M. D. Zeiler, D. Krishnan, G. W. Taylor, and R. Fergus, “Deconvolutional networks,” in *2010 IEEE Computer Society Conference on Computer Vision and Pattern Recognition*, 2010, pp. 2528–2535.
- [10] H. Yuan, H. Yu, S. Gui, and S. Ji, “Explainability in graph neural networks: A taxonomic survey,” *ArXiv*, vol. abs/2012.15445, 2020.
- [11] Z. Yu and H. Gao, “Motifexplainer: a motif-based graph neural network explainer,” *CoRR*, vol. abs/2202.00519, 2022. [Online]. Available: <https://arxiv.org/abs/2202.00519>
- [12] A. Duval and F. Malliaros, “Graphsvx: Shapley value explanations for graph neural networks,” in *European Conference on Machine Learning and Knowledge Discovery in Databases (ECML PKDD)*, 2021.
- [13] D. Luo, W. Cheng, D. Xu, W. Yu, B. Zong, H. Chen, and X. Zhang, “Parameterized explainer for graph neural network,” *Advances in Neural Information Processing Systems*, vol. 33, 2020.
- [14] R. Ying, D. Bourgeois, J. You, M. Zitnik, and J. Leskovec, “Gnnexplainer: Generating explanations for graph neural networks,” *Advances in neural information processing systems*, vol. 32, pp. 9240–9251, 12 2019.
- [15] M. N. Vu and M. T. Thai, “Pgm-explainer: Probabilistic graphical model explanations for graph neural networks,” *ArXiv*, vol. abs/2010.05788, 2020.
- [16] H. Yuan, J. Tang, X. Hu, and S. Ji, “Xggn: Towards model-level explanations of graph neural networks,” 08 2020, pp. 430–438.
- [17] J. Lee, R. Rossi, and X. Kong, “Graph classification using structural attention,” 07 2018, pp. 1666–1674.
- [18] D. Xu, W. Cheng, D. Luo, X. Liu, and X. Zhang, “Spatio-temporal attentive rnn for node classification in temporal attributed graphs,” 08 2019, pp. 3947–3953.
- [19] M. Zhang and Y. Chen, “Link prediction based on graph neural networks,” 02 2018.
- [20] T. N. Kipf and M. Welling, “Semi-supervised classification with graph convolutional networks,” in *International Conference on Learning Representations (ICLR)*, 2017.
- [21] J. Gilmer, S. Schoenholz, P. Riley, O. Vinyals, and G. Dahl, “Neural message passing for quantum chemistry,” 04 2017.
- [22] P. Veličković, G. Cucurull, A. Casanova, A. Romero, P. Liò, and Y. Bengio, “Graph Attention Networks,” *International Conference on Learning Representations*, 2018, accepted as poster. [Online]. Available: <https://openreview.net/forum?id=rJXMpikCZ>
- [23] H. Dai, Z. Kozareva, B. Dai, A. J. Smola, and L. Song, “Learning steady-states of iterative algorithms over graphs,” *Proc. of ICML*, p. 1114–1122, 2018.
- [24] K. Xu, W. Hu, J. Leskovec, and S. Jegelka, “How powerful are graph neural networks?” in *International Conference on Learning Representations*, 2019. [Online]. Available: <https://openreview.net/forum?id=ryGs6iA5Km>
- [25] Z. Wu, S. Pan, F. Chen, G. Long, C. Zhang, and P. Yu, “A comprehensive survey on graph neural networks,” *IEEE Transactions on Neural Networks and Learning Systems*, vol. PP, pp. 1–21, 03 2020.
- [26] P. Pope, S. Kolouri, C. Martin, and H. Hoffmann, “Explainability methods for graph convolutional neural networks,” 06 2019.
- [27] F. Baldassarre and H. Azizpour, “Explainability techniques for graph convolutional networks,” *ArXiv*, vol. abs/1905.13686, 2019.

- [28] H. Yuan, H. Yu, J. Wang, K. Li, and S. Ji, “On explainability of graph neural networks via subgraph explorations,” in *Proceedings of the 38th International Conference on Machine Learning (ICML)*, 2021, pp. 12 241–12 252.
- [29] R. Schwarzenberg, M. Hübner, D. Harbecke, C. Alt, and L. Hennig, “Layerwise relevance visualization in convolutional text graph classifiers,” *ArXiv*, vol. abs/1909.10911, 2019.
- [30] Q. Huang, M. Yamada, Y. Tian, D. Singh, D. Yin, and Y. Chang, “Graphlime: Local interpretable model explanations for graph neural networks,” *ArXiv*, vol. abs/2001.06216, 2020.
- [31] M. T. Ribeiro, S. Singh, and C. Guestrin, ““why should i trust you?”: Explaining the predictions of any classifier,” in *Proceedings of the 22nd ACM SIGKDD International Conference on Knowledge Discovery & Data Mining*, ser. KDD ’16. New York, NY, USA: Association for Computing Machinery, 2016, p. 1135–1144. [Online]. Available: <https://doi.org/10.1145/2939672.2939778>
- [32] A. Nguyen, J. Yosinski, and J. Clune, “Deep neural networks are easily fooled: High confidence predictions for unrecognizable images,” 06 2015, pp. 427–436.
- [33] E. N. Gilbert, “Random graphs,” *The Annals of Mathematical Statistics*, vol. 30, no. 4, pp. 1141–1144, 1959. [Online]. Available: <http://www.jstor.org/stable/2237458>
- [34] C. Maddison, A. Mnih, and Y. Teh, “The concrete distribution: A continuous relaxation of discrete random variables,” 11 2016.
- [35] K. Kersting, N. M. Kriege, C. Morris, P. Mutzel, and M. Neumann, “Benchmark data sets for graph kernels,” 2016. [Online]. Available: <http://graphkernels.cs.tu-dortmund.de>
- [36] A. K. Debnath, R. L. Lopez de Compadre, G. Debnath, A. J. Shusterman, and C. Hansch, “Structure-activity relationship of mutagenic aromatic and heteroaromatic nitro compounds. correlation with molecular orbital energies and hydrophobicity,” *Journal of Medicinal Chemistry*, vol. 34, no. 2, pp. 786–797, 1991. [Online]. Available: <https://doi.org/10.1021/jm00106a046>

A Regularization

In order to facilitate optimization and ensure that the explanation graphs are constrained to desired properties, we apply multiple regularization terms to the latent parameters.

$L1$ and $L2$ Regularization. $L1$ and $L2$ regularizations are widely used to encourage model sparsity and reduce the parameter size. In our case, both regularizations are applied on Ω during the optimization to reduce its size, with the purpose of mitigating the saturating gradient problem caused by the sigmoid function in Equation 7 from the manuscript. For $k \in \{1, 2\}$, L_k penalty term is defined as

$$R_{L_k} = \|\Omega\|_k. \quad (9)$$

Budget Penalty. Budget penalty is employed in instance-level GNN explanation methods (i.e., PGExplainer and GNNExplainer) to generate compact and meaningful explanations. For the model-level explanation, budget penalty can prevent the size of explanation graphs from growing unboundedly with repeated discriminative patterns. Budget penalty is defined as

$$R_b = \text{softplus}(\|\text{sigmoid}(\Omega)\|_1 - B)^2, \quad (10)$$

where B is the expected maximum number of edges in the explanation graph. Unlike PGExplainer, we utilize softplus instead of ReLU to slack the rate of gradient change near the boundary condition. In addition, the penalty is squared to further discourage extremely large graphs.

Connectivity Constraint. Inspired by PGExplainer, we apply a connectivity constraint to encourage explanation graphs to be connected, by minimizing the Kullback–Leibler divergence between the probabilities of each pair of edges that share a common node in the Gilbert random graph,

$$R_c = \sum_{i \in V} \sum_{j, k \in \mathcal{N}(i)} \text{D}_{\text{KL}}(P_{ij} \| P_{ik}) \quad (11)$$

where P_{ij} denotes the Bernoulli distribution parameterized by $\text{sigmoid}(\omega_{ij})$. As opposed to PGExplainer, KL-divergence is chosen over cross-entropy in order to decouple the entropy of individual edge distributions from the connectivity constraint.

B Experimental Setup

All the experiments are conducted on a single core of an Intel Core i9 CPU. Speaking of the software, all the models are implemented in Python 3.9. We use PyTorch 1.10 for auto-differentiation and numerical optimization. Besides, all the GNNs are implemented with PyTorch Geometric 2.0. We also use PyTorch-Scatter library to handle vector gather-scatter operations. Lastly, we utilize NetworkX for graph data generation and processing.

C Synthetic Dataset Generation

In the experimental study, we evaluate the efficacy of GNNInterpreter on 3 synthetic datasets: Cyclicity, Shape, and Motif. Among them, Cyclicity and Motif are synthetically generated on top of Rome Dataset¹ which has 11534 undirected graphs with 10-100 nodes. The generation procedures for all 3 synthetic datasets are specified in algorithm 2, algorithm 3, and algorithm 4, respectively.

Algorithm 2: Cyclicity dataset generation procedure

Edge Classes: {RED, GREEN}
Graph Classes: {RED-CYCLIC, GREEN-CYCLIC, ACYCLIC}
Input: Rome Dataset
Output: A collection of pairs consisted of a graph and its label

```
1 for  $G$  in Rome Dataset do
2   Randomly label each edge in  $G$  as RED or GREEN.
3   if  $G$  is acyclic then
4     yield ( $G$ , ACYCLIC)
5     break
6   end
7   while more than one cycle exists in  $G$  do
8     Remove a random edge from a random cycle in  $G$ .
9   end
10  Randomly pick a color  $C_{\text{cycle}} \in \{\text{RED}, \text{GREEN}\}$ .
11  Relabel all edges in the remaining cycle in  $G$  as  $C_{\text{cycle}}$ .
12  Randomly pick a color  $C_{\text{edge}} \in \{\text{RED}, \text{GREEN}\}$ .
13  Relabel a random edge in the remaining cycle in  $G$  as  $C_{\text{edge}}$ .
14  if  $C_{\text{cycle}} = C_{\text{edge}} = \text{RED}$  then
15    yield ( $G$ , RED-CYCLIC)
16  else if  $C_{\text{cycle}} = C_{\text{edge}} = \text{GREEN}$  then
17    yield ( $G$ , GREEN-CYCLIC)
18  else
19    yield ( $G$ , ACYCLIC)
20  end
21 end
```

D Experimental Details of GNN Classifiers

In the experimental study, we adopt GNNInterpreter to explain 4 GNN classifiers which are trained on 4 different datasets. In this section, we will describe some experimental details about the GNN models for all 4 datasets. These experimental details include the model architecture, hyper-parameter settings, and test F1 scores per class obtained by the GNN models.

D.1 MUTAG

The GNN classifier we implemented for MUTAG dataset is a deep GCN model that contains 3 GCN layers of width 64, a global mean pooling layer, and 2 dense layers in the end. The model uses LeakyReLU as activation. Before training, the model parameters are initialized with Kaiming initializer. During training, AdamW optimizer is used for optimization with learning rate of 0.01 and weight decay of 0.01. The F1 scores for two classes in Table 4 shows that the GNN is more accurate when making decisions on Mutagen class.

¹<http://www.graphdrawing.org/data.html>

Algorithm 3: Motif dataset generation procedure

Node Classes: {RED, GREEN, ORANGE, BLUE, MAGENTA}**Graph Classes:** {HOUSE, HOUSE-X, COMPLETE-4, COMPLETE-5, OTHERS}**Input:** Rome Dataset**Output:** A collection of pairs consisted of a graph and its label

```
1 Let  $\{G_{\text{HOUSE}}, G_{\text{HOUSE-X}}, G_{\text{COMPLETE-4}}, G_{\text{COMPLETE-5}}\}$  be 4 motifs for the corresponding classes.
2 Define  $\oplus$  as a graph operator such that  $G_1 \oplus G_2$  generates a union graph  $G_1 \cup G_2$  with an additional
  edge between a random node in  $G_1$  and a random node in  $G_2$ .
3 for  $G$  in Rome Dataset do
4   Randomly select a label  $L \in \{\text{OTHERS}, \text{HOUSE}, \text{HOUSE-X}, \text{COMPLETE-4}, \text{COMPLETE-5}\}$ .
5   if  $L = \text{OTHERS}$  then
6     Let  $G_{\text{OTHERS}}$  be a random motif in  $\{G_{\text{HOUSE}}, G_{\text{HOUSE-X}}, G_{\text{COMPLETE-4}}, G_{\text{COMPLETE-5}}\}$  but with a random
      edge being removed.
7   end
8   yield  $(G \oplus G_L, L)$ 
9 end
```

Algorithm 4: Shape dataset generation procedure

Graph Classes: {LOLLIPOP, WHEEL, GRID, STAR, OTHERS}**Output:** A collection of pairs consisted of a graph and its label

```
1 for 8000 times do
2   Randomly select a label  $L \in \{\text{OTHERS}, \text{LOLLIPOP}, \text{WHEEL}, \text{GRID}, \text{STAR}\}$ .
3   switch  $L$  do
4     case LOLLIPOP do
5       Sample lollipop graph  $G_{\text{LOLLIPOP}}$  with random number of head nodes  $n \in \{4, \dots, 16\}$  and
        random number of tail nodes  $m \in \{4, \dots, 16\}$ .
6     case WHEEL do
7       Sample wheel graph  $G_{\text{WHEEL}}$  with random number of non-center nodes  $n \in \{4, \dots, 64\}$ .
8     case GRID do
9       Sample grid graph  $G_{\text{GRID}}$  with random width  $w \in \{2, \dots, 8\}$  and random height  $h \in \{2, \dots, 8\}$ .
10    case STAR do
11      Sample star graph  $G_{\text{STAR}}$  with random number of non-center nodes  $n \in \{4, \dots, 64\}$ .
12    case OTHERS do
13      Sample Binomial random graph  $G_{\text{OTHERS}}$  with random number of nodes  $n \in \{8, \dots, 32\}$  and
        random edge probability  $p \in [0.2, 1]$ .
14    end
15    Add random number of noisy edges to  $G_L$  with a random ratio  $p \in [0, 0.2]$ .
16    yield  $(G_L, L)$ 
17 end
```

D.2 Cyclicity

The GNN classifier for Cyclicity dataset is a deep NNConv model that contains 5 NNConv layers of width 32 with a single-layered edge network, a global mean pooling layer, and 2 dense layers in the end. Before training, the model parameters are initialized with Kaiming initializer. During training, AdamW optimizer is used for optimization with learning rate of 0.01, learning rate decay of 0.01, and weight decay of 0.01. As shown in Table 4, all three classes have similar F1 scores, which means that the GNN model have a balanced performance on each class.

D.3 Motif

The Motif dataset uses exactly the same model architecture and hyper-parameter settings as MUTAG dataset. The F1 score per class presented in Table 4 indicates that the GNN achieves a perfect performance on Complete-5 class and a near-perfect performance on every other classes.

D.4 Shape

The Shape dataset uses the same model architecture and hyper-parameter settings as MUTAG dataset except that the model contains 4 GCN layers instead of 3 GCN layers. Also, the F1 score per class

in Table 4 shows that the GNN can perfectly predict the Star class, whereas the predictions for the Lollipop class and the Grid class are less accurate.

Table 4: The F1 score per class of the corresponding GNN classifiers for all datasets.

Dataset	F1 Scores of GNN Classifier			
MUTAG	Mutagen	Nonmutagen		
	0.961	0.917		
Cyclicity	Red Cyclic	Green Cyclic	Acyclic	
	0.995	0.992	0.993	
Motif	House	House-X	Complete-4	Complete-5
	0.998	0.998	0.996	1.000
Shape	Lollipop	Wheel	Grid	Star
	0.969	0.994	0.966	1.000

Table 5: The regularization weights of GNNInterpreter for explaining the GNN models corresponding to each dataset.

Dataset	Class	Regularization Weights			
		R_{L_1}	R_{L_2}	R_b	R_c
MUTAG	Mutagen	10	5	20	1
	Nonmutagen	5	2	10	2
Cyclicity	Red Cyclic	10	5	10000	100
	Green Cyclic	10	5	2000	50
	Acyclic	10	2	5000	50
Motif	House	1	1	5000	0
	House-X	5	2	2000	0
	Complete-4	10	5	10000	1
	Complete-5	10	5	10000	5
Shape	Lollipop	5	5	1	5
	Wheel	10	5	10	0
	Grid	1	1	2	0
	Star	10	2	200	0

E Experimental Details of GNNInterpreter

For all experiments, we choose to set the Concrete Distribution temperature $\tau = 0.2$. We use the sample size $K = 10$ for all Monte Carlo samplings. For optimization, we adopt SGD optimizer with the learning rate of 1 and terminate the learning procedure until convergence. Additionally, in the training objective, the embedding similarity weight μ is set to 1 for every dataset except MUTAG. For MUTAG dataset, we let $\mu = 10$ due to its nature that the structure of the graphs in the dataset needs to follow certain domain-specific rules. A higher value of μ allows the GNNInterpreter to implicitly capture these rules from the average graph embeddings. Speaking of the regularization weight, we employ grid search to obtain the best results under different combinations of regularization terms. To ensure the reproducibility of our experimental results, we also report the exact regularization weights used for the quantitative and qualitative evaluation in the manuscript (see Table 5). Note that we adopt a constant weight strategy for L1 regularization R_{L_1} , L2 regularization R_{L_2} , and connectivity constraint R_c throughout the training process. In contrast, for budget penalty R_b , we employ a 500-iteration initial warm up period to gradually increase the weight starting from 0.

F An Ablation Study of the Second Term in Objective Function

In many cases, the second term in the objective function (see Equation 2 from the manuscript) plays a significant role in generating meaningful explanations. To assess the effectiveness of the second term, we take MUTAG dataset as an example to conduct an ablation study on this term. Given that our explanation graph of the non-mutagen class does not reveal any specific pattern (see Figure 1 from

the manuscript), the effect of the second term on explaining non-mutagen class might not be obvious. Therefore, we will only compare the explanation with or without the second term for the mutagen class, which is shown in Figure 3. Given the same color codes used in the manuscript, we can see that the explanation without the second term completely deviates from the true data distribution. The known discriminative feature of the mutagen class (i.e., NO₂) even do not appear at all in the explanation without the second term. Even though the logits of the explanation without the second term are significantly higher than the logits of the explanation with the second term, it is difficult to gain the meaningful insights from the explanation without the second term. The result of this ablation study emphasizes the importance of the second term, especially for the classifications task involving domain-specific knowledge. Also, we may conclude that the out-of-distribution explanation graph might not provide meaningful insight on how the model actually reasons over the true data distribution, which is what we actually care about.

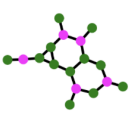
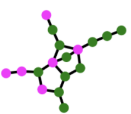
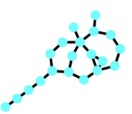
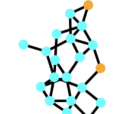
	with second term		without second term	
Explanation Graphs				
Logits	43.45	34.98	310.14	286.42

Figure 3: The explanation graphs of the mutagen class generated with or without second term for the GNN trained with MUTAG dataset. For each category (column), there are 2 explanation graphs along with the corresponding class score before softmax (logits).

G A Verification Study of Our Analysis about Qualitative Results

From Figure 1 in the manuscript, the explanation graphs for some classes are different from the true graphs in the training data, which might indicate the potential pitfall of the explained GNN. However, since the ground truth model-level explanation graph does not exist, it is difficult to verify the correctness of our analysis regarding these potential pitfalls. In this section, we conducted the controlled experimental studies for MUTAG, House-X in Motif and Complete-4 in Motif, to verify our high-level interpretation of the explained GNN mentioned in the manuscript.

G.1 Motif

For Complete-4 class in Motif dataset, we believe that the discriminative feature the GNN tries to detect is that "every node should have 3 neighbors in different color". This rule is concluded from our observation of the commonality between our explanation graph and the ground truth motif. We found 8 different motifs (including the ground truth Complete-4) which satisfy this rule, as shown in Figure 4. Given a fixed set of 5000 Rome graphs, these 8 different motifs are attached to the same node of those 5000 Rome graphs. As a result, we obtain 8 sets of graphs, and each set includes 5000 graphs corresponding to a single motif. For each motif set, the average predicted class probability of each class and the total number of graphs which are classified as each class are presented in the Table 6 and Table 7, respectively. We can clearly see that motif 1-6 successfully fool the explained GNN because their predicted class probability of Complete-4 is significantly higher than their predicted class probability of Others. This results also indicate that our previous analysis regarding how the GNN makes prediction for Complete-4 is correct. The GNN trained with the Motif dataset might misclassify the graphs containing a motif satisfying the rule that "every node should have 3 neighbors in different color" to the Complete-4 class.

For House-X class in the Motif dataset, we speculate the true belief inside the explained GNN is that "orange node and red node should have 3 neighbors except purple node, green node and blue node should have 4 neighbors in different color". This discriminative feature is also deduced from the commonality between our explanation for House-X and the ground truth motif. The 9 motifs satisfying this rule are shown in Figure 5. The controlled experimental study for House-X class is conducted in a similar manner as for Complete-4 class. The quantitative results for each motif set in Table 9 and Table 10 shows that all the plausible motifs satisfying the rule are highly likely to be

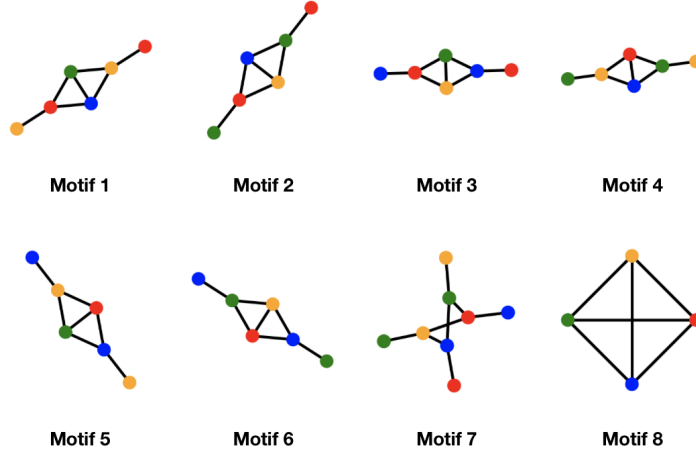


Figure 4: Plausible Complete-4 motifs. The motifs satisfying the rule that every node should have 3 neighbors in different color. The motif 8 is the ground truth Complete-4 motif. The ground truth class label of motif 1-7 should be the Others class.

	Motif 1	Motif 2	Motif 3	Motif 4	Motif 5	Motif 6	Motif 7	Motif 8 (GT)
Others	0.4123	0.4064	0.4122	0.4033	0.4116	0.4019	0.9974	0.0066
House	0.0000	0.0000	0.0000	0.0000	0.0000	0.0000	0.0021	0.0000
House-X	0.0002	0.0006	0.0004	0.0007	0.0003	0.0002	0.0001	0.0000
Complete-4	0.5875	0.593	0.5874	0.596	0.5881	0.5978	0.0004	0.9934
Complete-5	0.0000	0.0000	0.0000	0.0000	0.0000	0.0000	0.0001	0.0000

Table 6: The quantitative results of plausible Complete-4 motifs. For each motif set (column), the average predicted class probability of each class (row) is computed by averaging over 5000 graphs containing the corresponding motif.

	Motif 1	Motif 2	Motif 3	Motif 4	Motif 5	Motif 6	Motif 7	Motif 8 (GT)
Others	2030	1983	2016	1985	2031	1966	4994	0
House	0	0	0	0	0	0	4	0
House-X	1	3	1	4	1	1	0	0
Complete-4	2969	3014	2983	3011	2986	3033	2	5000
Complete-5	0	0	0	0	0	0	0	0

Table 7: The classification results of plausible Complete-4 motifs. For each motif set (column), the total number of graphs which are classified as the classes (row) is presented in this table. The sum of all columns should be 5000 because that is the total number of graphs in each motif set.

classified as House-X, no matter what are their corresponding ground truth labels. Specifically, a large number of graphs from motif set 1-8 are misclassified to the House-X class, especially the motif 1 and motif 6. It also indicates that the GNN are easily fooled by the graphs containing the plausible motifs satisfying the rule that "orange node and red node should have 3 neighbors except purple node, green node and blue node should have 4 neighbors in different color". In summary, speaking of the GNN trained with Motif dataset, our explanation results remind people to be cautious when applying this GNN to classify some unseen graphs containing those plausible motifs.

	Motif 1	Motif 2	Motif 3	Motif 4	Motif 5	Motif 6	Motif 7	Motif 8	Motif 9 (GT)
Others	0.2929	0.4411	0.3558	0.3849	0.4317	0.1296	0.3351	0.3373	0.0022
House	0.0000	0.0000	0.0000	0.0000	0.0000	0.0000	0.0000	0.0000	0.0000
House-X	0.7053	0.5581	0.6435	0.6144	0.5678	0.8700	0.6641	0.6620	0.9978
Complete-4	0.0002	0.0003	0.0004	0.0004	0.0004	0.0003	0.0008	0.0007	0.0000
Complete-5	0.0016	0.0004	0.0002	0.0003	0.0002	0.0001	0.0000	0.0000	0.0000

Table 8: The quantitative results of plausible House-X motifs. For each motif set (column), the average predicted class probability of each class (row) is computed by averaging over 5000 graphs containing the corresponding motif.

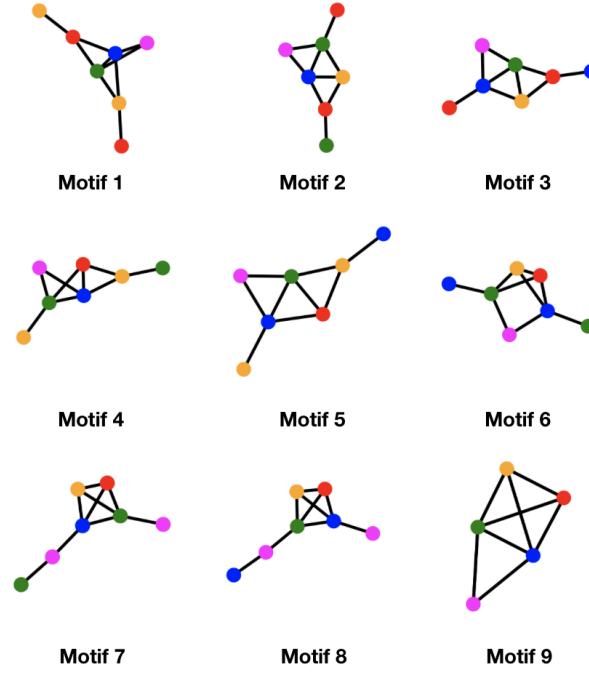


Figure 5: Plausible House-X motifs. The motifs satisfying the rule that orange node and red node should have 3 neighbors except purple node, green node and blue node should have 4 neighbors in different color. The motif 9 is the ground truth House-X motif. The ground truth class label of motif 1-8 should be the Others class.

	Motif 1	Motif 2	Motif 3	Motif 4	Motif 5	Motif 6	Motif 7	Motif 8	Motif 9 (GT)
Others	0.2929	0.4411	0.3558	0.3849	0.4317	0.1296	0.3351	0.3373	0.0022
House	0.0000	0.0000	0.0000	0.0000	0.0000	0.0000	0.0000	0.0000	0.0000
House-X	0.7053	0.5581	0.6435	0.6144	0.5678	0.8700	0.6641	0.6620	0.9978
Complete-4	0.0002	0.0003	0.0004	0.0004	0.0004	0.0003	0.0008	0.0007	0.0000
Complete-5	0.0016	0.0004	0.0002	0.0003	0.0002	0.0001	0.0000	0.0000	0.0000

Table 9: For each motif set, the average predicted class probability of each class is computed by averaging over 5000 graphs containing the corresponding motif.

	Motif 1	Motif 2	Motif 3	Motif 4	Motif 5	Motif 6	Motif 7	Motif 8	Motif 9 (GT)
Others	1434	2251	1808	1970	2183	597	1682	1696	10
House	0	0	0	0	0	0	0	0	0
House-X	3566	2749	3192	3030	2817	4403	3318	3304	4990
Complete-4	0	0	0	0	0	0	0	0	0
Complete-5	0	0	0	0	0	0	0	0	0

Table 10: The classification results of plausible House-X motifs. For each motif set (column), the total number of graphs which are classified as the classes (row) is presented in this table. The sum of all columns should be 5000 because that is the total number of graphs in each motif set.

G.2 MUTAG

According to the explanation graphs provided in Figure 1 from the manuscript, the discriminative feature captured by our explanation graph for the mutagen class is the occurrences of the NO2 group. However, there are no special pattern observed from our explanation graph for the non-mutagen class. To verify whether the occurrences of NO2 group is truly the discriminative feature GNN tries to detect when making prediction for the mutagen class, we designed a controlled experiment such that each set of graphs contains different numbers of NO2 group while keeping other experimental settings the same. To be specific, given 1000 randomly generated Gabriel graphs with 5-10 nodes, each time we attach 15 nodes to these random graphs. These 15 nodes will be divided into 5 groups, and each group has 3 nodes. The frequency of NO2 group appearing in these 15 nodes varies from 0 to 5. For instance, in Figure 6, the example graph for 5 NO2 contains a Gabriel graph with 6 nodes and 5 NO2 groups; the example graph for 4 NO2 contains the same Gabriel graph, 4 NO2 groups, and a random group of 3 nodes. As a result, we will obtain 6 sets of graphs and each set includes 1000 graphs containing a fixed number of NO2 group.

Then, we feed these 6000 graphs into the GNN trained with the MUTAG dataset to obtain the quantitative results. Similar to what we did for Motif dataset, for each 1000 graphs with a fixed number of NO2 group, the average predicted class probability for each class and the number of graphs being classified as each class is presented in Table 11 and Table 12. We can clearly see that as more and more NO2 group occurs, the GNN is more certain about predicting these graphs as the mutagen class. We can infer that the NO2 groups indeed are the discriminative features the GNN tries to detect when making prediction for the mutagen class, which is also consistent to our finding when analyzing our explanations for both classes. It is interesting to observe that the GNN seems bias toward the non-mutagen class unless the GNN finds enough evidence (i.e., NO2 group) for the mutagen class. It may indicate that this GNN suffers from the bias attribution issue so that no special pattern is observed from our explanation graph for non-mutagen class.

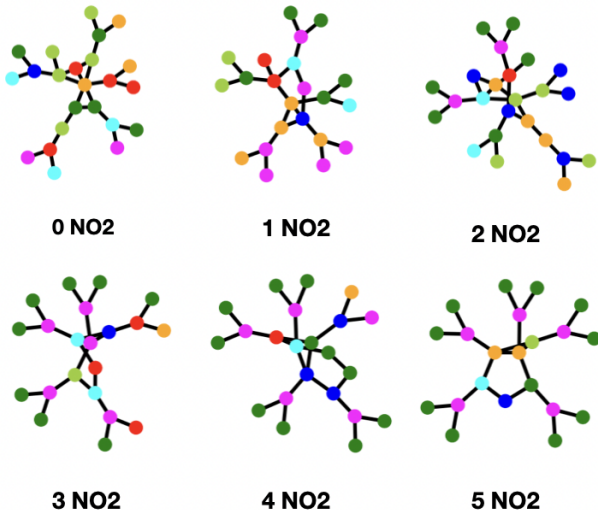


Figure 6: The example graphs with different numbers of NO2 groups attached to the same Gabriel graph with 6 random nodes.

H The Evaluation Results of Is_Acyclic from XGNN

In order to conduct more comprehensive comparison with the baseline method, we managed to test our work on Is_Acyclic which is posted at XGNN GitHub². We trained a GCN model to do the classification task with an accuracy of 0.9789 and adopted GNNInterpreter to explain the two

²<https://github.com/divelab/DIG/tree/main/dig/xgraph/XGNN>

15 Nodes	0 NO ₂	1 NO ₂	2 NO ₂	3 NO ₂	4 NO ₂	5 NO ₂
Non-Mutagen	0.9837	0.9651	0.9186	0.7593	0.3998	0.0714
Mutagen	0.0163	0.0349	0.0814	0.2407	0.6002	0.9286

Table 11: The quantitative results of graphs with different numbers of NO₂ groups. For each 1000 graphs with the fixed number of NO₂ groups (column), the average predicted class probability of each class (row) is computed by averaging over 1000 graphs containing the fixed number of NO₂ group.

15 Nodes	0 NO ₂	1 NO ₂	2 NO ₂	3 NO ₂	4 NO ₂	5 NO ₂
Non-Mutagen	984	965	917	758	396	71
Mutagen	16	35	83	242	604	929

Table 12: The classification results of graphs with different numbers of NO₂ groups. For each 1000 graphs with the fixed number of NO₂ groups (column), the number of graphs being classified as the classes (row) is presented. The sum of all columns should be 1000.

classes in Is_Acyclic. The quantitative and qualitative evaluation of GNNInterpreter on Is_Acyclic is conducted in a similar fashion of Table 2 from the manuscript.

However, it is unfortunate that XGNN could not provide any meaningful explanation for the GCN model we trained with Is_Acyclic (like what we experienced for the Shape and Motif dataset). We spent an extensive amount of time tuning the hyper-parameter of XGNN, but we still did not get meaningful and acceptable explanation graphs within the limited time frame. We also attempted to conduct a comparative study on the GNN model trained by the XGNN authors because its model checkpoint is available in the google drive folder they shared. But unfortunately, the model definition of the GNN model on Is_Acyclic is not available on GitHub (only the model definition of GNN on MUTAG is provided on their GitHub) so we cannot successfully load the GNN checkpoint. Therefore, the quantitative and qualitative evaluation of XGNN on the GCN model we trained with Is_Acyclic is not presented in section G. It is worth mentioning that in the XGNN paper, they presented multiple explanation graphs for the GNN model they trained on Is_Acyclic. Please feel free to check it out.

Speaking of the evaluation results, the quantitative results in Table 13 shows that all explanation graphs generated by GNNInterpreter are classified correctly with almost 100% probability for both classes. That is to say, our explanation graph can serve as a good representative for both classes. Besides, the explanation graphs presented in Figure 7 are consistent with the class definition without differing from the true graphs in the training data.

Table 13: The quantitative results for Is_Acyclic. As the quantitative metric, we compute the average class probability of 1000 explanation graphs and the standard deviation of them for the two classes. In addition, the average training time per class of training 100 different GNNInterpreter is also included for efficiency evaluation.

Dataset [Method]	Predicted Class Probability by GNN		Training Time Per Class
Is_Acyclic [Ours]	Cyclic	Acyclic	20 s
	0.999 \pm 0.001	1.000 \pm 0.000	


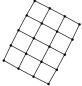


Dataset [Method]	Generated Model-Level Explanation Graphs			
Is_Acyclic [Ours]	Cyclic		Acyclic	
				
	explanation	example	explanation	example

Figure 7: The qualitative results for Is_Acyclic. For each class in all datasets, the explanation graph with the class probability of 1 predicted by the GNNs is displayed on the left; as a reference, the example graph selected from the training data of the GNNs is displayed on the right.

I Multiple Qualitative Examples Per Class Per Dataset

For each dataset, multiple qualitative examples per class are shown in Figure 8

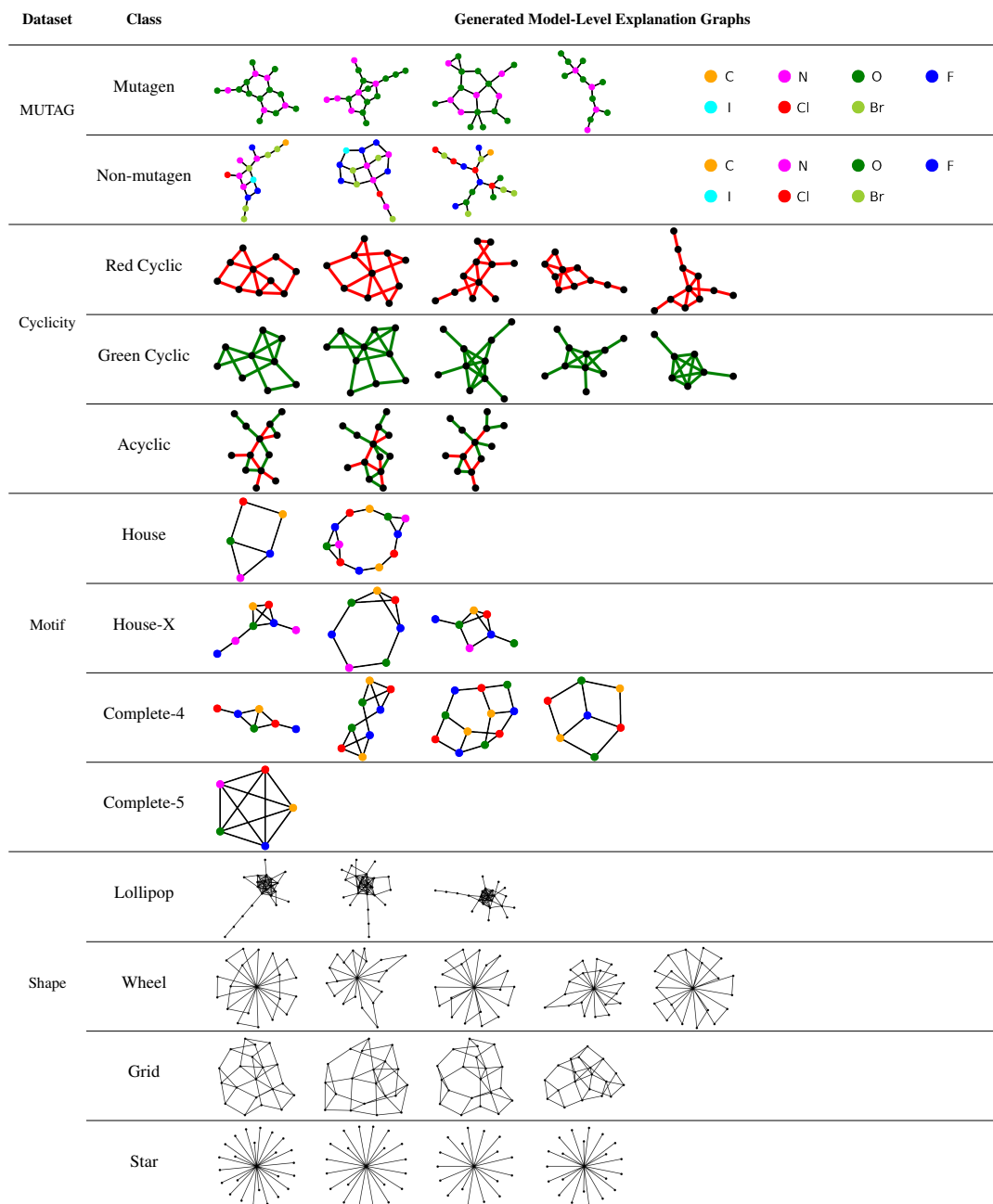


Figure 8: The qualitative results for 4 datasets. For each class in all datasets, multiple explanation graphs with the class probability of 1 predicted by the GNNs is displayed. If the dataset has the node feature or edge feature, the different colors in the nodes and edges correspondingly represent different values in the node feature and edge feature.